2014 IEEE International Conference on Robotics & Automation (ICRA)
Hong Kong Convention and Exhibition Center
May 31 - June 7, 2014. Hong Kong, China

Self-Stable One-Legged Hopping Using a Curved Foot

Fabian Günther[1,2], Fabio Giardina[1,2] and Fumiya Iida[1]

Abstract— **Reduction of the system complexity is currently one of the main challenges for efficient and versatile legged robot locomotion. In this paper, we present a new one legged hopping robot called CHIARO, which is equipped with a curved foot. Even though the robot has no sensory feedback and consists of only two rigid bodies and one spring loaded joint with parallel actuation, it is able to achieve stable forward-hopping over a wide range of parameters and forward-speeds. Operating at natural hopping frequency, the parallel actuation shows good efficiency. This paper presents an approach to determine stability and efficiency of a highly non-linear mechanical system. By implementing a two dimensional numerical model, taking into account ground contact forces by a Newtonian kinematic impact- and coulomb friction law, we conducted a thorough parameter analysis based on a series of simulations. The comparison of the simulation and real world experiments shows good accordance, which qualifies the simulation for parameter optimization including prediction of robot stability and efficiency.**

I. INTRODUCTION

The musculoskeletal body plan of legged animals combines both efficiency and high versatility. The small size of a single body cell compared to the overall structure results in a high total number of these basic functional units. Therewith optimized lightweight and versatile components of high complexity can be realized. Accordingly most of today's versatile legged robots have also a high grade of complexity to be able to solve their tasks, even if the functional range is small compared to biological systems. But for machines in general, high complexity leads to high design, manufacturing and operational effort and the high number of moving parts lowers the overall efficiency due to mechanical interaction. In addition, the high number of parameters complicates a proper system analysis or makes it even impossible. On the other side of the spectrum, simple and/or efficient robots suffer from a narrow range of flexibility and are mostly constrained to flat ground.

Considering efficiency, versatility and complexity for legged robot locomotion, three groups of robots can be distinguished. On the side of the efficient locomotors as the first group, today's actuated passive dynamic walkers are able to achieve bipedal walking at the same level of animal's energy efficiency [1]. By optimizing the robot for a certain operational area, the combination of high performance and high efficiency is possible [2]. Although an adaption to different slopes is possible, these robots are restricted to relatively uniform ground and their mechanism shows a high grade of complexity. By taking advantage of free vibration, curved beam hoppers [3] are able to achieve similar efficiency with clearly reduced complexity. The second group covers high versatile robots designed on the one hand as flexible test and demonstration platforms [4] or for specific mission profiles like transportation in rough terrain [5] or testing of human equipment [6]. Complexity and efficiency are of minor matter. The third group contains robots that are efficient, versatile and simple at the same time. By including electric motors and series elasticity, versatile robots were made more efficient [8]. By adding extra features like walking in circles, efficient robots were made more versatile [9]. By combining the mechanics of wheeled robots with compliant legs, complexity of legged robots was reduced [7].

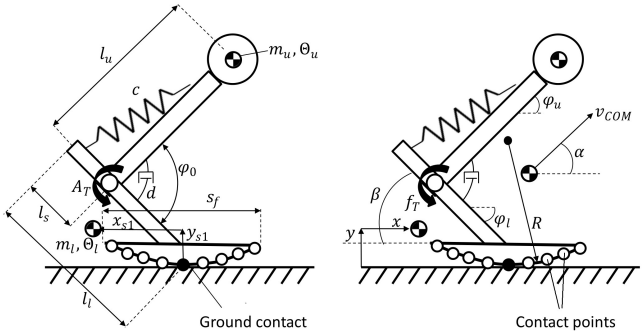

Fig. 1. Illustration of the physical model used for the simulations. It consists of two rigid bodies (lower and upper leg), which are connected with a spring loaded and damped rotational joint. On the joint, a parallel motor torque is applied.. The lower leg is attached to a curved foot which establishes ground contact during stance phase. The foot is discretized by placing 10 contact points uniformly on the outer arc of the foot. During rolling motion in stance either one or two contact points establish ground contact.

As a contribution to this third group of robots, we combined the simple mechanics of a two segmented one legged hopper with a curved foot. This approach minimizes the number of parameters which simplifies the analysis. The goal of this paper is to show that this set up can guarantee stable hopping gaits over a wide range of parameters while achieving a good overall efficiency. Further we introduce some first parameter connections to tune the robots forward-speed and efficiency.

We structure the rest of the paper as follows. Section II describes the basic design and physical modelling of the

*This study was supported by the Swiss National Science Foundation Grant No. PP00P2123387/1 and the Swiss National Science Foundation through the National Centre of Competence in Research Robotics.

[1]F. Günther, F. Giardina and F. Iida are with Bio-Inspired Robotics Lab, Institute of Robotics and Intelligent Systems, ETH Zurich, Leonhardstrasse 27, 8092 Zurich, Switzerland, fabiangu@ethz.ch, fabiogi@ethz.ch, fumiya.iida@mavt.ethz.ch

[2] Both authors contributed equally to this publication.

TABLE I

PARAMETERS AND VARIABLES OF THE ROBOT MODEL USED FOR SIMULATIONS

Fixed Parameters		
Letter	**Name**	**Value and Unit**
c	Spring stiffness	$3022\,\mathrm{N\,m^{-1}}$
d	Damping coefficient	$0.06\,\mathrm{N\,m\,s}$
l_l	Lower body length	$0.2\,\mathrm{m}$
l_u	Upper body length	$0.16\,\mathrm{m}$
l_s	Moment arm spring	$0.05\,\mathrm{m}$
m_l	Lower body mass	$0.239\,\mathrm{kg}$
m_u	Upper body mass	$0.481\,\mathrm{kg}$
A_T	Motor torque amplitude	$0.5\,\mathrm{N\,m}$
s_f	Foot length	$0.2\,\mathrm{m}$
x_{s1}	Horizontal coordinate of lower leg center of mass	$-0.063\,\mathrm{m}$
y_{s1}	Vertical coordinate of lower leg center of mass	$0.045\,\mathrm{m}$
θ_l	Lower body inertia	$0.0015\,\mathrm{kg\,m^2}$
θ_u	Upper body inertia	$0.0016\,\mathrm{kg\,m^2}$
φ_0	Initial Knee angle for relaxed spring	$0.7853\,\mathrm{rad}$
Tunable Parameters		
f_T	Motor torque angular frequency	$2\,\mathrm{Hz}$ to $6\,\mathrm{Hz}$
R	Foot Radius	$0.2\,\mathrm{m}$ to $0.6\,\mathrm{m}$
β	Lower leg angle	$0.4\,\mathrm{rad}$ to $1.2\,\mathrm{rad}$
Variables		
$x(t)$	Position x-value of lower leg COM	m
$y(t)$	Position y-value of lower leg COM	m
$\varphi_l(t)$	Lower leg angle	rad
$\varphi_u(t)$	Upper leg angle	rad
Computed Variables		
$T_M(t)$	Motor moment function	N m
$\alpha(t)$	Take-off angle of the Center of Mass (COM)	rad
$\varphi(t)$	Knee angle	rad
$\omega_T(t)$	Motor torque angular velocity	$\mathrm{rad\,s^{-1}}$

robot. The simulation set up is explained in section III while section IV presents simulation results on stability, efficiency and parameter interaction. Section V describes a series of real world experiments to confirm the simulation results and section VI concludes the paper with some remarks on future works.

II. DESIGN AND MODELING

To explore the behavior of a curved foot on a one legged hopping robot, we started with a simulation to establish the basic characteristics and to find suitable sets of parameters. In parallel, we developed the CAD model of the real robot to guarantee a good grade of accordance with the simulation.

A. Physical Model

The planar robot model we use is shown in figure 1. It consists of two rigid bodies, a foot and an upper part. The bodies are connected with a rotational joint on which a linear push/pull spring is attached. Joint friction is modelled by linear rotational damping in the joint. A curved foot is attached to the lower leg to ensure ground contact during stance phase. On the joint, a parallel motor torque is applied. Note that the motor inertia is neglected.

B. Parameters

As a starting point, the motor (a Maxon EC45-flat with $70\,\mathrm{W}$ and a total weight of $141\,\mathrm{g}$) and the robot size (around $0.3\,\mathrm{m}$ height) was given. From the conceptual side, the drive belt gear with ratio 1:12.75, the two segmented body and the curved foot was set. To reduce the number of parameters, we decided to constrain the system. First, The curved foot is designed as a circle segment with constant radius. Second, the motor is placed on top of the upper body on the same point where the push-pull spring is attached. Due to the fact that motor and motor plate represent the majority of the upper body mass, we assumed that the center of mass of the upper body concides with the motor position. Fourth, the lower leg is attached to the middle of the curved foot. Finally, the motor torque input is constant during the run is sinusoidal

$$T_t(t) = r \cdot \sin(\omega_T \cdot t) \tag{1}$$

with $\omega_T = f_T \cdot 2\pi$. This leads to the given set of 17 parameters shown in table I. Due to mechanical design issues (see section V-A), we chose the frequency f_T, the foot radius R and the lower leg angle β to be our tuning parameters. The remaining parameters were set as constant based on first simulations where some suitable parameter sets were established.

C. Control Strategy

The simulation, as well as the real robot, are feed forward controlled without any sensory feedback. All stabilization pitching motion is achieved by exploiting the intrinsic dynamics of the mechanical structure. The stabilization around the x-axis of the experimental platform is achieved mechanically using two foot plates with a distance of $0.2\,\mathrm{m}$ in z-direction.

D. Hopping Pattern

At touchdown, the robot touches the ground with the curved part of the foot. During stance phase, the foot is rolling forward and the knee first bends and then flexes. At take-off, the foot stands either on the curved area or on the front foot tip, depending on the parameter set for the run. During flight phase, the knee bends again while the hopper swings back to its landing position.

III. SIMULATION SETUP

A. Ground Contact Model

Due to ground contact interactions, namely friction- and impact forces, the robot shows properties of a non-smooth mechanical system. The equations of motion for our system are depending on the minimal coordinates

$$\vec{q} = \begin{pmatrix} x & y & \varphi_l & \varphi_u \end{pmatrix}^T. \tag{2}$$

The mathematical equations of motion of our system

$$\mathbf{M}\,\ddot{\mathbf{q}}(\mathbf{q}, t) - \mathbf{h}(\mathbf{q}, \dot{\mathbf{q}}, t) = 0, \tag{3}$$

can be extended by the contact forces as proposed in [10]. This leads to the following measure equality for a dynamical system

$$\mathbf{M}\,\mathrm{d}\mathbf{u} - \mathbf{h}\,\mathrm{d}t - \mathrm{d}\mathbf{R} = 0, \tag{4}$$

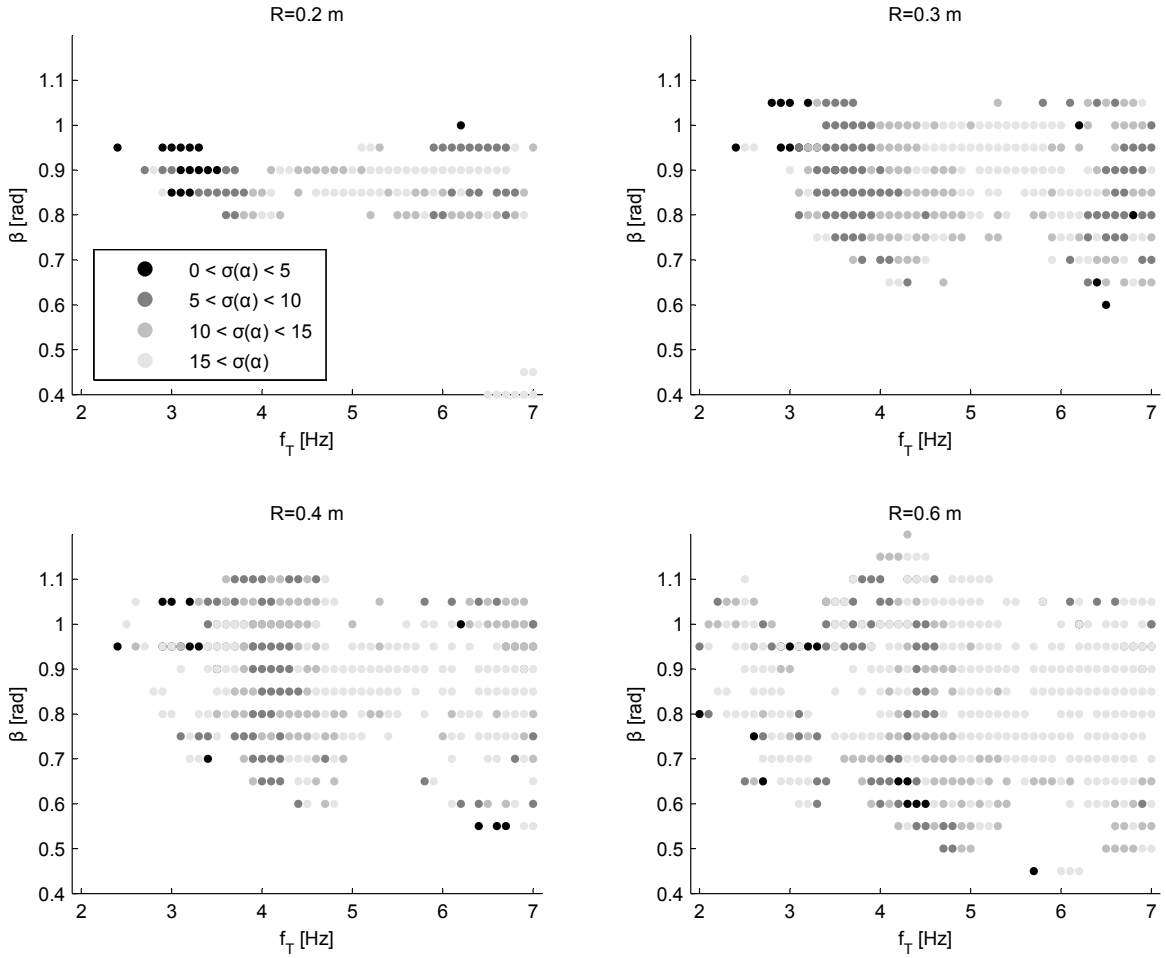

Fig. 2. Standard deviation plots of α from simulation data as a function of motor frequency f_T and lower leg angle β for different foot radii R. For all radii, the whole frequency and angle range was simulated. Each dot indicates a successful run, which means not falling down during the runtime of 5s. White areas imply unsuccessful runs. Every run starts from static rest position. Amplitude and frequency were hold constant during each run.

where $\mathbf{M}$ is the mass matrix, $\mathbf{u}$ is the velocity of the system in minimal coordinates, $\mathbf{h}$ are the gyroscopic accelerations as well as smooth, generalized forces and $\mathrm{d}\mathbf{R}$ is the measure of the contact forces. By defining force laws for $\mathrm{d}\mathbf{R}$, which depend on the system's kinematic states, it is possible to set up an optimization problem (linear complementarity problem) for our contact forces. In our case, we assumed a newtonian impact behavior, which has the form

$$v_N^+ = -\varepsilon_N \, v_N^-, \qquad v_T^+ = -\varepsilon_T \, v_T^-, \tag{5),(6}$$

where v_N^+ is the normal velocity of the colliding body just before impact, ε_N is the restitution factor in normal direction and v_N^- is the velocity of the colliding body right after the impact. The same holds for the tangential direction to the contact, which is labelled with the subscript T. In our physical model, we assumed that the restitution number in normal and tangential direction is equal to zero, as no energy should be recovered from the unsprung mass. For the forces in tangential direction, we assumed a coulomb friction model with equal static and dynamic friction coefficient. Once the solution of the optimization problem is found, we can re-enter the contact forces in eq. (4) and integrate normally.

With this method, it is not necessary to switch the basic differential equations between ground phase and flight phase, as the properties of our system are altered by Lagrangian multipliers.

For our robot, we implemented a time stepping algorithm in order to solve the described system numerically. The curved foot was discretized by placing multiple contact points uniformly on the outer arc of the foot. Claiming that maximally two contact points of the convex foot can be touching the flat ground simultaneously, the numerical effort to solve the optimization problem is manageable and can be executed with a reasonable performance using an enumerative method.

B. Simulation Environment

The crucial parameters for the ground interaction are the friction coefficients and the normal- and tangential restitution factors, respectively. As for the first, we assumed a friction coefficient of 0.3 throughout the simulation for all contact points. For the restitution factors, we chose all to be equal to zero for all contact points, which corresponds to a complete dissipation of kinetic energy of the unsprung mass at impact.

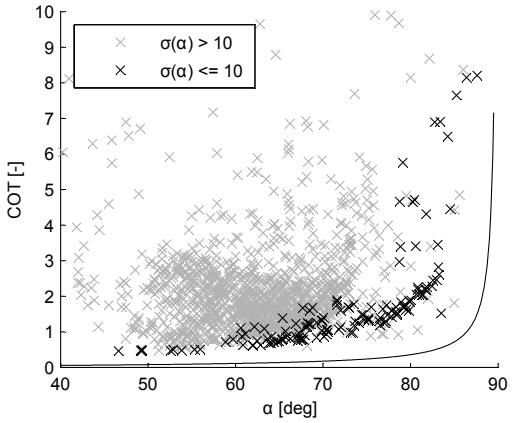

Fig. 3. Simulated cost of transport as a function of the take-off angle α of the lower leg. The continuous black line indicates the minimum cost of transport possible for a hopping mass with coefficient of impact $\varepsilon = 0.5$. The parameter set used was the same used for figure 2. The lowest cost of transport is 0.458 with $f_T = 2.9\,\text{Hz}, R = 0.3\,\text{m}, \beta = 1.05\,\text{rad}$. Runs with $\sigma(\alpha) < 10$ contain at least 10 hops.

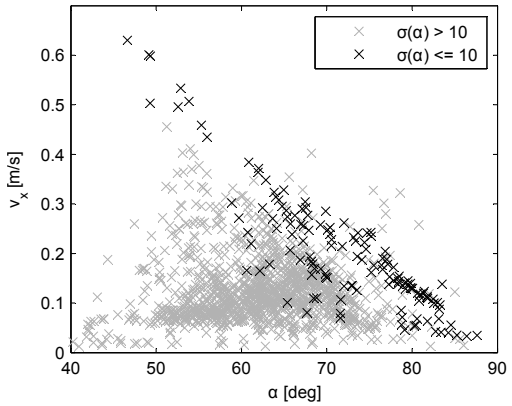

Fig. 4. Forward-speed as a function of the take-off angle α. The highest forward-speed is $0.63\,\text{m}\,\text{s}^{-1}$ with $f_T = 2.9\,\text{Hz}, R = 0.3\,\text{m}, \beta = 1.05\,\text{rad}$. Runs with $\sigma(\alpha) < 10$ contain at least 10 hops.

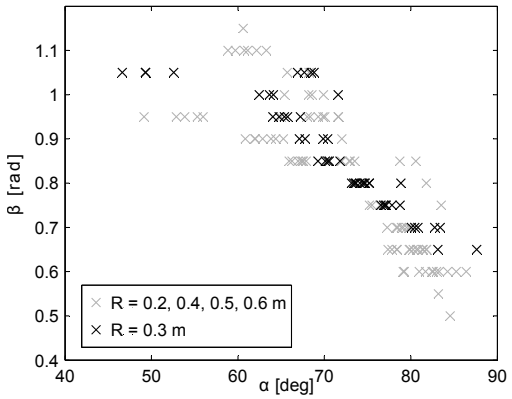

Fig. 5. Simulated relation between take-off angle α and lower leg angle β for different foot radii R. Runs with $\sigma(\alpha) < 10$ contain at least 10 hops.

For each simulation, the initial conditions were precalculated in order to start from the robot's static equilibrium position. As a consequence, the same initial conditions as for the real world experiment could be guaranteed. However, static stability became a necessary condition for a successful run.

As the simulation requires that maximally two contact points are touching the ground, the integration time step Δt has to be chosen sufficiently small, such that the foot does not immerse in the ground. This problem occurred primarily when a low curvature of the foot arc and a high number of contact points were chosen. We limited the contact point number to $n = 10$ to overcome this problem instead of increasing the integration step number. With set $\Delta t = 0.0005\,\text{s}$, the simulations showed only insignificant changes of the results when fewer contact points were applied to the foot.

IV. SIMULATION RESULTS

We performed several simulations to test both stability and efficiency of the curved foot hopper concept. The parameters f_T, R, β were varied between the runs (see section II), the other parameters were kept constant. Due to the fact that the system is highly non-linear and good stability measures are not easily found, we used the following stability indicators:

1) Every set of parameters that guarantees a run of $5\,\text{s}$ accelerating from deadlock without falling down we call successful.
2) We use the standard deviation of the take-off angle α as an indicator for the system stability. The lower the standard deviation, the better the system stability.

A. Stability

In a first experiment, we explored the robot's behavior for different foot radii R, angular frequencies f_T and foot angles β. It turned out that successful hopping on flat ground is possible for a wide range of geometric parameters, input energy and speed. The results of the experiment are shown in figure 2.

First, it can be seen that the parameter range for successful runs is larger at larger foot radius R. While there are successful runs for each angular frequency f_T independent from the foot radius, the range of successful runs for different lower leg angles increases with increasing foot radius. A possible explanation for this behavior is founded in the fact that larger foot radii lead to larger distances between the foot circle center point and the center of mass. This results in increased raising moments. Second, the standard deviation of the take-off angle α indicates high stability of motion at lower frequencies. For $R = 0.2\,\text{m}$ it shows a clear link between high cost of transport, low take-off angle α and low standard deviation of α. For $R = 0.6\,\text{m}$, this connection does not exist.

B. Cost Of Transport And Forward-Speed

In a second experiment we explored the parameter influence on the forward-speed and on the efficiency of locomotion, indicated by the cost of transport (COT). The cost of transport is defined as follows

$$COT = \frac{E_{in}}{m \cdot g \cdot s} \tag{7}$$

with the input energy E_{in}, the robot mass m, the gravitational acceleration g and the travelled distance s. For the simulation, we calculate the input energy out of the joint torque during the whole run including accelerating from deadlock

$$E_{in} = \int_{\varphi_1}^{\varphi_2} T_M(t) \cdot d\varphi \tag{8}$$

Motor, Motor Controller and Gearbox losses are neglected in this experiment.

Figure 3 shows the average costs of transport for the same set of parameters used for figure 2. The best COT was 0.458 achieved with the parameter set $f_T = 2.9\,\mathrm{Hz}, R = 0.3\,\mathrm{m}, \beta = 1.05\,\mathrm{rad}$. Figure 4 shows the corresponding average forward-speed. The highest forward-speed achieved was $0.63\,\mathrm{m\,s^{-1}}$ with the parameter set of the lowest cost of transport.

It can be seen that runs with a low standard variation of the take-off angle α show both the highest forward-speed and the lowest cost of transport with respect to the jumping angle. A steady and continuous hopping motion is a direct hint for low cost of transport. This fact is very useful for (automatic) parameter tuning.

While the area for high cost of transport and low forward-speed is extensive, the sharp edge at low cost of transport and high forward-speed indicates a theoretical limit for the two parameters. For the minimum cost of transport depending on the take-off angle α we can formulate a relation as follows

$$COT_{min} = \frac{1}{4}(1 - \varepsilon_N)^2 \tan(\alpha) \tag{9}$$

For this function we assumed that only the vertical element of the velocity is lossy due to impact losses determined by the normal restitution coefficient ε_N. The horizontal element of the velocity is assumed to be lossless which is equal to no friction during stance phase. An ideal foot rolling motion would correspond to this assumption.

Figure 5 shows a nearly linear connection between the lower leg angle β and the resulting take-off angle α. While α directly determines the forward-speed (see figure 4), this result qualifies β as a direct control parameter for the forward-speed.

V. REAL WORLD EXPERIMENT

The CAD model of the real world robot was developed in parallel with the simulations to guarantee a good grade of consistency. In addition, we chose the parameters to vary based on the mechanical constraints, this means we only varied parameters in the simulation for which the modification on the real robot is easy.

A. Experimental Platform

The curved foot hopper CHIARO is shown in figure 6. Upper and lower leg of the robot were made of carbon tubes with a ball bearing knee joint out of 3D print material. This design approach guarantees lightweight and stiff parts with a high grade of modularity and low manufacturing time. The foot is realized using two plywood plates which are screwed to the lower leg. A distance of $0.2\,\mathrm{m}$ guarantees a save stand and prevents the robot from falling to the side. The manufacturing of the plates is easy and fast, so different foot radii and lower leg angles can be realized by changing the foot plates. The joint torque is generated with a brushless outrunner motor (Maxon EC45 flat, 70 W) and transmitted with a timing belt drive. The drive has a gear ratio of 1:12.75, the main Pulley is connected to the lower leg. The push-pull spring of the simulation model is realized using two opposed pull-springs with half of the spring stiffness. The motor mount with the counter bearing to hold the tension of the pulley is made of aluminium. An encoder is mounted on the motor shaft to enable precise tracking of the motor position and knee angle. The whole robot (except the motor mount) can be manufactured and assembled within two days. The motor is torque controlled using a MAXON Escon 50/5 motor driver and a PC with MATLAB. The motor wires are guided in a long loop above the robot to minimize the influence of wiring mass.

Fig. 6. Picture of the curved foot hopper CHIARO used for the experiments. All parameters are identical to the model used for the simulations. The joint torque is generated by a brushless outrunner motor (Maxon EC45 flat, 70 W) and transmitted with a timing belt drive. The drive has a gear ratio of 1:12.75, the main Pulley is connected to the lower leg. Screwed plywood footplates allow easy change of foot radius R and lower leg angle β. The push-pull spring of the simulation model is realized using two opposed pull-springs with half of the spring stiffness.

Absent any inertial sensing on CHIARO, we used an OptiTrack optical tracking system to record the robot's position and orientation. Due to high noise, the visual tracking data was filtered using a Gaussian filter.

B. Simulation Tuning And Accordance Analysis

In a first experiment, we tested the accordance between simulation and real robot. We chose several successful parameter sets out of the simulation (see section IV-A) and repeated the run with the real robot with identical parameter set up according to table I. Based on this data we performed a fine tuning of the damping coefficient and friction, while all other simulation parameters were left constant. The results are shown in figure 7. For low standard deviations of α the data shows an excellent accordance between simulated and experimental values. For higher standard deviations, the basic behavior is still well mapped. Due to more and more chaotic behavior of the robot, the data differs during the acceleration phase.

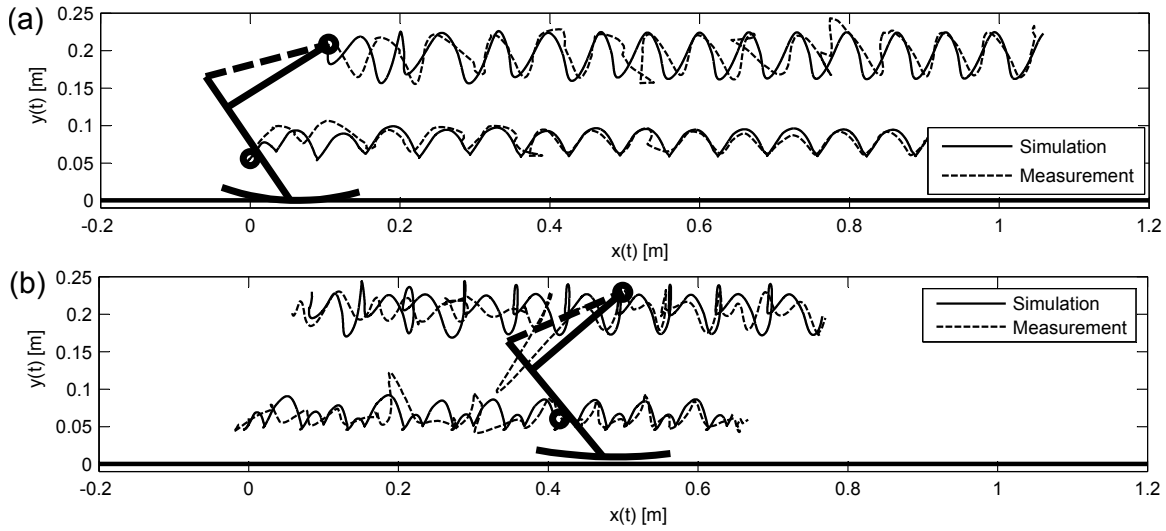

Fig. 7. Trajectory of upper and lower COM for simulated and experimental runs. The parameters were set according to table I. (a) shows a run with low standard variation of α with $f_T = 3.4\,\text{Hz}, R = 0.3\,\text{m}, \beta = 1.05\,\text{rad}$. The accordance between experiment (dotted line) and simulation (continuous line) is excellent, the anomalies especially for the upper COM are founded in high noise of the optical tracking system. (b) shows a run with high standard deviation of α with $f_T = 4.3\,\text{Hz}, R = 0.6\,\text{m}, \beta = 0.9\,\text{rad}$. The speedup phase of the robot differs between simulation and experiment, but after a few hops at final speed the motion stabilizes and the accordance is good. The anomalies especially for the upper COM are again founded in high noise of the optical tracking system.

The accordance of the standard deviation between simulation and experiment was very high for every run performed, so the simulation seems to be a good tool to predict the standard deviation for future runs with other parameter sets. Due to this fact we believe that the simulation can be used for both, subsequent analysis of the real robot behavior as well as prediction of future robot behavior, as long as the standard deviation of the analyzed run is low enough.

VI. CONCLUSION

This paper investigated a novel one legged hopper that takes advantage of a curved foot. The system is feed forward controlled, all stabilization is done mechanically. Among others, this paper specifically investigated the influence of the curved foot approach on stability and efficiency over a wide range of parameters and forward velocities. By keeping the experimental platform as simple as possible, we were able to describe the system with a high grade of accuracy. By analyzing the robots behavior using numerical analysis, we were able to gain insights in the interaction of the system parameters and their influence on stability and efficiency and identified stable regions of parameters. We identified the foot angle as a direct determining factor for the hopping angle and thus for the achievable forward-speed. By comparing the simulation with the experiments, we determined excellent accordance which verifies the simulation and empowers it for both, explanation and prediction of robot behavior.

In the future we continue more comprehensive analysis on system borders (max. speed and min. CoT) and exploration on parameter interaction with the target to explore the underlying mechanisms of the robots self stabilizing properties.

REFERENCES

[1] S. Collins, A. Ruina, R. Tedrake, and M. Wisse. Efficient bipedal robots based on passive dynamic walkers, Science 307, 2005, 1082-1085.

[2] S. Cotton, I. Mihai, V. Olaru, M. Bellman, T. van der Ven, J. Godowski, and J. Pratt. FastRunner: A Fast, Efficient and Robust Bipedal Robot. Concept and Planar Simulation, IEEE International Conference on Robotics and Automation, Saint Paul, Minnesota, USA, 2012.

[3] M. Reis, and F. Iida. Hopping Robot Based on Free Vibration of an Elastic Curved Beam, IEEE/ASME International Conference on Advanced Intelligent Mechatronics (AIM), Budapest, Hungary, 2011.

[4] Y. Sakagami, R. Watanabe, C. Aoyama, S. Matsunaga, N. Higaki, and K. Fujimura. The intelligent asimo: System overview and integration, in Proc. IEEE/RSJ Int. Conf. on Intelligent Robots and Systems (IROS02), 2002, pp. 2478-2483.

[5] M. Raibert, K. Blankespoor, G. Nelson, and R. Playter. Bigdog, the rough-terrain quadrupet robot, Proceedings of the 17th World Congress, The International Federation of Automatic Control, Seoul, Korea, 2008.

[6] G. Nelson, A. Saunders, N. Neville, B. Swilling, J. Bondaryk, D. Billings, C. Lee, R. Playter, and M. Raibert, M. PETMAN: A Humanoid Robot for Testing Chemical Protective Clothing, Journal of the Robotics Society of Japan Vol. 30 (2012) No. 4 pp. 372-377.

[7] U. Saranli, M. Buehler and D.E. Koditschek, RHex: A Simple and Highly Mobile Hexapod Robot, The International Journal of Robotics Research July 2001 vol. 20 no. 7 pp. 616-631.

[8] M. Hutter, C. Gehring, M. Bloesch, M.A. Hoepflinger, C.D Remy, and R. Siegwart, StarlETH: A compliant quadrupedal robot for fast, efficient, and versatile locomotion, 15th International Conference on Climbing and Walking Robot - CLAWAR 2012, Johns Hopkins University, USA.

[9] P.A. Bhounsule, J. Cortell, and A. Ruina, Design and Control of Ranger: An Energy-Efficient, Dynamic Walking Robot, CLAWAR 2012 Proceedings of the Fifteenth International Conference on Climbing and Walking Robots and the Support Technologies for Mobile Machines, Baltimore, MD, USA, 2012.

[10] C. Glocker, and C. Studer, Formulation and Preparation for Numerical Evaluation of Linear Complementarity Systems in Dynamics, Multibody System Dynamics, Springer-Verlag 2005, pp. 447-463.